The cytoplasmic adaptor protein X11α and extracellular matrix protein Reelin regulate ApoE receptor 2 trafficking and cell movement

S. Sakura Minami,* You Me Sung,† Sonya B. Dumanis,* Seong Hwan Chi,* Mark P. Burns,* Eun-Jung Ann,‖ Toshiharu Suzuki,¶ R. Scott Turner,‡ Hee-Sae Park,‖ Daniel T. S. Pak,§ G. William Rebeck,* and Hyang-Sook Hoe*,[1]

*Department of Neuroscience, †Department of Oncology, ‡Department of Neurology, and §Department of Pharmacology, Georgetown University Medical Center, Washington, District of Columbia, USA; ‖Hormone Research Center, School of Biological Sciences and Technology, Chonnam National University, Gwangju, Republic of Korea; and ¶Laboratory of Neuroscience, Graduate School of Pharmaceutical Sciences, Hokkaido University, Sapporo, Japan

ABSTRACT **The goal of this study was to determine the effect of X11α on ApoE receptor 2 (ApoEr2) trafficking and the functional significance of this interaction on cell movement in MCF 10A epithelial cells. We found that X11α increased surface levels of ApoEr2 by 64% compared to vector control, as determined by surface protein biotinylation. To examine the functional significance of this effect, we tested whether ApoEr2 played a novel role in cell movement in a wound-healing assay. We found that overexpression of ApoEr2 in MCF 10A cells increased cell migration velocity by 87% ($P<0.01$, $n=4$) compared to GFP control. Cotransfection of X11α had an additive effect on average velocity compared to ApoEr2 alone (13%; $P<0.05$, $n=4$). In addition, we tested whether ApoEr2 ligands altered the effect of ApoEr2 on cell movement. We found that treatment with concentrated medium containing the extracellular matrix protein Reelin, but not control medium, further increased the velocity of ApoEr2- but not APP-transfected cells (20%; $P<0.001$, $n=4$). Similarly, Reelin treatment increased cell velocity in the presence of ApoEr2 and X11α (10%; $P<0.05$, $n=4$). In the present study, we are the first to demonstrate that ApoEr2 regulates cell movement, and both X11α and Reelin enhance this effect.—Minami, S. S., Sung, Y. M., Dumanis, S. B., Chi, S. H., Burns, M. P., Ann, E.-J., Suzuki, T., Turner, R. S., Park, H.-S., Pak, D. T. S., Rebeck, G. W., Hoe, H.-S. The cytoplasmic adaptor protein X11α and extracellular matrix protein Reelin regulate ApoE receptor 2 trafficking and cell movement. *FASEB J.* 24, 58–69 (2010). www.fasebj.org**

Key Words: Mint · wound healing · cell migration

ALZHEIMER'S DISEASE (AD) is an age-related neurodegenerative disease characterized by progressive deterioration of memory and cognitive function, which is highly correlated with loss of synapses followed by cell death (1). The pathogenesis of AD is associated with the aggregation of Aβ peptide, a fragment of the β-amyloid precursor protein (APP). The most prominent genetic risk factor for late-onset AD is apolipoprotein E (APOE) (2). The APOE gene encodes the soluble apoE protein, which transports cholesterol and other lipids in the plasma and cerebrospinal fluid (3). ApoE interacts with a family of apoE receptors, which mediate endocytosis of their ligands *via* their NPXY sequences, followed by recycling to the cell surface (4).

We and others have found that APP and ApoE receptors share a number of common intracellular binding proteins, including Dab1, FE65, and X11 (5–8). Each of these adaptor proteins affects the trafficking and processing of their bound proteins. Dab1 is known to affect neuronal migration downstream of APP (9), and interactions between APP and Dab1 are known to be important for brain development in *Drosophila* (10). Dab1 also acts downstream of Reelin, an extracellular matrix molecule, which regulates neuronal migration and neurite outgrowth during development (9, 11–14). FE65 binds both APP and ApoEr2 and affects their trafficking and processing. In addition, the interaction between FE65 and APP accelerates cell migration in a wound-healing assay through binding of FE65 to Mena, an actin-binding cytoskeletal protein (15). FE65 also binds the APP intracellular domain (AICD) and initiates transcriptional activation through trafficking of AICD to the nucleus (16, 17).

The X11 family of adaptor proteins also interacts with ApoEr2, as well as APP. The X11 family members, X11α, -β, and -γ (also referred to as Mint 1, 2, and 3), contain a PTB domain and two PDZ domains (18). X11α and X11β affect APP trafficking and processing (19–21), and the X11α interaction with ApoEr2 may

[1] Correspondence and current address: Department of Neurology, Georgetown University, 4000 Reservoir Rd. NW, Washington, DC 20057, USA. E-mail: hh69@georgetown.edu

doi: 10.1096/fj.09-138123

0892-6638/10/0024-0058 © FASEB

induce ApoE-mediated endocytosis of ApoEr2 in N2a-APPswe cells (22). Functionally, APP and ApoEr2 are known to be involved in neuronal development, and both interact with X11α. Therefore, we hypothesize that X11α may also contribute to these processes.

In the present study, we demonstrate that ApoEr2 interacts with X11α and increases ApoEr2 cell-surface levels in MCF 10A cells. Interestingly, Reelin treatment altered the intracellular binding between ApoEr2 and X11α in a time-dependent manner, and also decreased X11α-mediated tyrosine phosphorylation of ApoEr2. We further show a novel role for ApoEr2 in accelerating cell migration in a wound-healing assay and the ability of both X11α and Reelin to enhance this effect. These data suggest an important role for both the extracellular matrix molecule Reelin and the intracellular adaptor protein X11α in the regulation of ApoEr2-mediated cell motility.

MATERIALS AND METHODS

Vector construction

ApoEr2 C-terminal constructs with HA tags were generated as described previously (23): ApoEr2 exon 18 only, ApoEr2 exon 19 only, and ApoEr2 exons 18 and 19 only. We also produced full-length ApoEr2 constructs with either an N-terminal or C-terminal GFP tag. We generated Flag-tagged deletion constructs of X11: X11α PDZ domain (residues 648-837), X11α PTB domain (residues 457–643), X11α PTB and PDZ domains (residues 457–837), Flag-tagged full-length X11α, and Flag-tagged full-length X11β. For X11β constructs, we generated X11β PDZ domain (residues 560–660) and the X11β PTB and PDZ domains (residues 368–660), which were each cloned into a pBHA vector that contained the LexA DNA-binding domain. Recombinant DNA was confirmed by sequencing, and expression of correctly sized proteins was confirmed by Western blot analysis.

Full-length Flag-tagged ApoEr2 construct lacking exon 19 was obtained from Joachim Herz (University of Texas Southwestern Medical Center, Dallas, TX, USA). A mixture of 3 siRNA sequences (siGENOME SMARTpool) targeted against human X11α (APBA1) was purchased from Dharmacon (Lafayette, CO, USA).

Yeast 2-hybrid system

The ApoEr2 C-terminal fragment (CTF) and X11α and X11β constructs were transformed into yeast strain L40. The histidine-selected yeast was grown on synthetic medium at 30°C for 3 d. Colonies were screened by X-gal filter assay and scored according to β-galactosidase expression time. ApoEr2 CTF domain (residues 757-870) was cloned into pGAD10 (Clontech, Mountain View, CA, USA), which has a GAL4 transcriptional activation domain as prey.

Cell lines and culture conditions

COS7 cells and MCF 10A cells were maintained as described previously (24). COS7 or MCF 10A cells were transiently transfected with 0.5–1 μg of plasmid in FuGENE6 (Roche, Nutley, NJ, USA), according to the manufacturer's protocol and cultured for 24 h in DMEM containing 10% FBS. Reelin-conditioned medium or control medium was prepared from either a stable cell line (HEK293) expressing Reelin or normal HEK293 cells. Medium was collected and concentrated by centrifugation at 4000 *g* for 20 min using Amicon Ultra filter devices (Millipore, Billerica, MA, USA). Immunoprecipitations were conducted with relevant antibodies as described previously (7, 8).

Antibodies

We used antibodies anti-HA (Abcam, Cambridge, MA, USA), anti-Mint1/X11α (BD Biosciences, San Jose, CA, USA; Sigma, St. Louis, MO, USA; Santa Cruz Biotechnologies, Santa Cruz, CA, USA), anti-Flag (Sigma), monoclonal Dab1 (Dr. Andre Goffinet, Catholic University of Leuven, Brussels, Belgium), anti-FE65 (Dr. Suzanne Guenette, Massachusetts General Hospital, Charlestown, MA, USA), anti-GFP (Invitrogen, Carlsbad, CA, USA), β-actin (Chemicon, Temecula, CA, USA), anti-ApoEr2 (Sigma), Fyn (Calbiochem, San Diego, CA, USA), and anti-c-myc (Abcam).

Primary neuronal culture

Hippocampal and cortical neurons from embryonic day 18 and 19 Sprague-Dawley rats were cultured at 150 cells/mm^2 as described previously (25).

Biotin-labeled cell-surface proteins

MCF 10A cells were transiently transfected as described above. After 24 h, surface proteins were biotin labeled, quenched, lysed, sonicated, and clarified by centrifugation, as described previously (7, 8). To isolate biotin-labeled proteins, lysate was incubated with immobilized NeutrAvidin TM Gel and was washed and incubated 1 h with SDS-PAGE sample buffer, including 50 mM DTT. Eluates were analyzed for ApoEr2 by immunoblotting.

Wound-healing assay

MCF 10A cells were transfected with indicated constructs using Lipofectamine 2000 (Invitrogen), and the medium was replaced with control or Reelin-conditioned medium 6 h later; then monolayers of cells were scratched using a fine pipette tip and immediately placed in a Nikon TE300 time-lapse microscope (Nikon, Tokyo, Japan). Time-lapse imaging was controlled using the Multidimensional Analysis tool of MetaMorph image acquisition software (Universal Imaging Corp., Center Valley, PA, USA). Gap width was determined at 0, 8, 16, and 24 h. Representative images are shown at 0 and 24 h. In a separate experiment, the velocity of cell migration was determined for individual cells using the Metamorph Image Analysis "Track Points" application. Data are represented as means ± SE and analyzed using 2-way ANOVA with Bonferroni post-test for gap width and 1-way ANOVA with Bonferroni post-test for velocity measures.

Statistical analyses

All data were analyzed using Student's *t* test or ANOVA with GraphPad Prism 4 software (GraphPad, San Diego, CA, USA), using Tukey's multiple-comparison test for *post hoc* analyses with significance determined as $P < 0.05$, unless otherwise stated. Descriptive statistics were calculated with StatView 4.1 (Abacus Concepts Inc., Berkeley, CA, USA) and are expressed as means ± SE.

RESULTS

X11α and X11β interact with ApoEr2

To test whether X11α interacts with ApoEr2, we transfected COS7 cells with ApoEr2 alone, both ApoEr2 and X11α, or X11α alone. We immunoprecipitated ApoEr2 with anti-HA or X11α with anti-Flag, and probed with anti-Flag for X11α or anti-HA for ApoEr2. Full-length X11α coprecipitated with ApoEr2 (**Fig. 1*A, B***). Western blot analysis of COS7 cell extracts confirmed that levels of total ApoEr2 and X11α were consistent across transfections (Fig. 1*A, B*). Similarly, we also tested whether another X11 family member, X11β, interacted with ApoEr2 in COS7 cells. Full-length X11β coprecipitated with ApoEr2 (Fig. 1*C, D*), while total levels of ApoEr2 and X11β were consistent across transfections (Fig. 1*C, D*).

To test whether endogenous ApoEr2 and X11α interacted, we immunoprecipitated primary neurons with anti-ApoEr2 or an irrelevant control antibody (α-P-JNK) and probed the precipitates with anti-X11α (Fig. 1*E*), or immunoprecipitated with anti-X11α or α-P-JNK and probed for ApoEr2 (Fig. 1*F*). Endogenous ApoEr2 and X11α coprecipitated, and no coprecipitation was detected in experiments performed with the control antibody. Immunoprecipitation of ApoEr2 from mouse brain lysates also resulted in coprecipitation of X11α

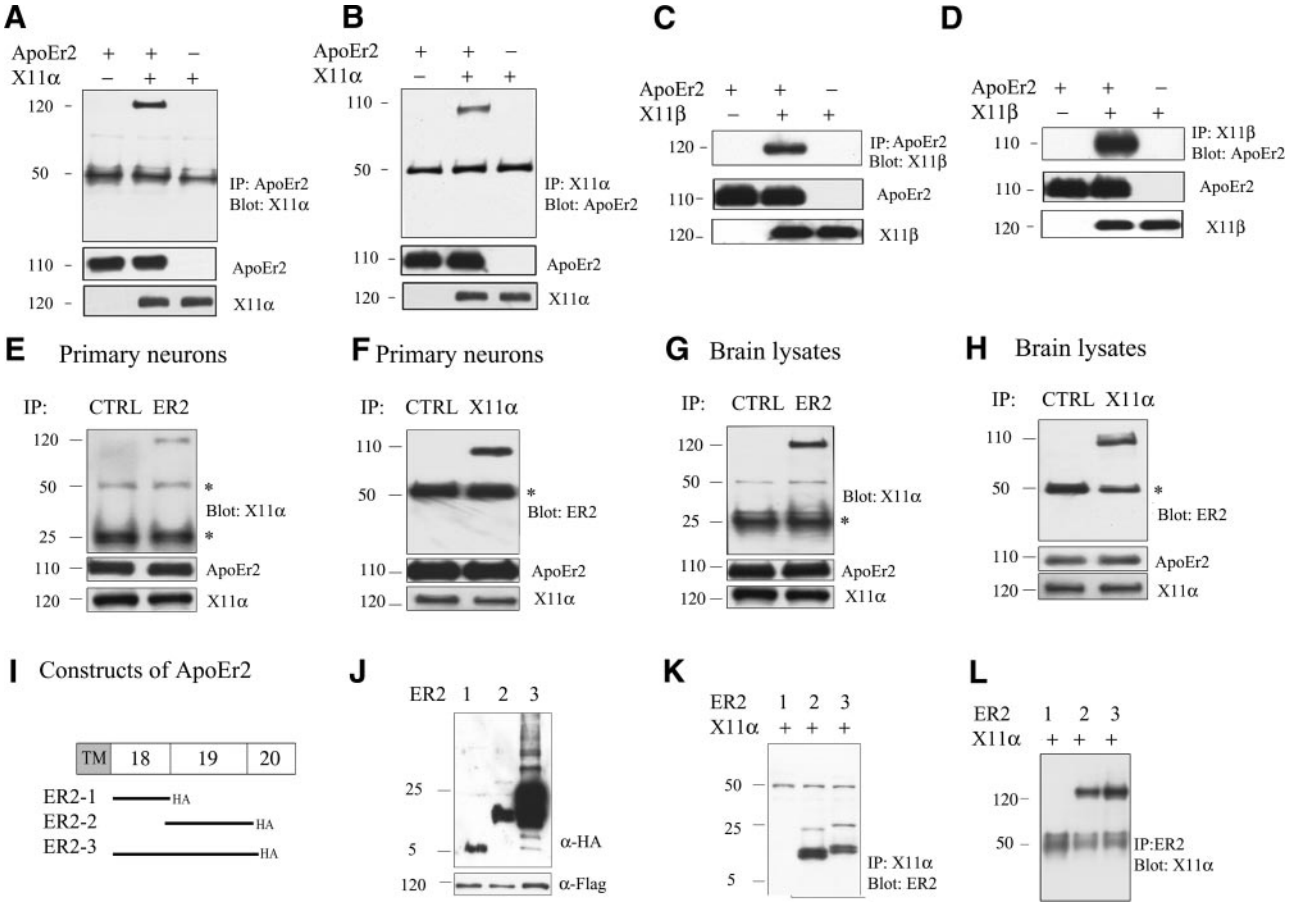

Figure 1. X11α and X11β interact with ApoEr2 in COS7 cells, in primary neurons, and brain, *via* exon 19 of ApoEr2. *A, B*) COS7 cells were transiently transfected with ApoEr2-HA, ApoEr2-HA and X11α-Flag, or X11α-Flag. Cell lysates were immunoprecipitated with HA and probed with anti-Flag ($n=3$) (*A*) or immunoprecipitated with anti-Flag and probed with anti-HA ($n=3$) (*B*). X11α and ApoEr2 coprecipitated. *C, D*) COS7 cells were transfected with ApoEr2, ApoEr2 and X11β, or X11β. Cell lysates were immunoprecipitated with anti-HA and probed with anti-Flag ($n=3$) (*C*), or immunoprecipitated with anti-Flag and probed with anti-HA ($n=3$) (*D*). ApoEr2 and X11β coprecipitated. Immunoblot of cell lysates showed similar levels of ApoEr2 and X11α or ApoEr2 and X11β (middle and bottom panels). *E, F*) Primary cortical neurons were immunoprecipitated with anti-ApoEr2 and probed with anti-X11α (*E*), or with anti-X11α and probed with anti-ApoEr2 ($n=3$) (*F*). As a negative control, the experiment was conducted with an irrelevant antibody (CTRL). *G, H*) Mouse brain lysates were immunoprecipitated with ApoEr2 antibody and probed with anti-X11α (*G*), or with X11α antibody and probed with anti-ApoEr2 ($n=3$) (*H*). An irrelevant antibody was used as negative control (CTRL). Bottom panels show total levels of proteins in lysates. Asterisks denote IgG heavy/light chains. *I*) Constructs of ApoEr2 with C-terminal HA tags containing exon 18 (ER2-1), exon 19 (ER2-2), and exon 18 and 19 (ER2-3). *J*) Cell lysates from COS7 cells transfected with indicated constructs were probed with anti-HA to demonstrate protein expression. *K, L*) COS7 cells were transfected with full-length X11α and ApoEr2 constructs as indicated. Cell lysates were immunoprecipitated with anti-Flag antibody and probed with anti-HA antibody ($n=2$) (*K*) or immunoprecipitated with anti-HA antibody and probed with anti-Flag antibody ($n=2$) (*L*).

and *vice versa*. The control antibody did not precipitate either X11α or ApoEr2 (Fig. 1*G, H*).

ApoEr2 exon 19 interacts with X11α

To test which domain of ApoEr2 interacts with X11α, we generated HA-tagged constructs of ApoEr2 C-terminal domains consisting of exon 18, exon 19, or both exons 18 and 19 (Fig. 1*I*). We cotransfected COS7 cells with ApoEr2 constructs and X11α. Expected protein sizes were expressed from each construct, as determined by Western blot (Fig. 1*J*). We then immunoprecipitated X11α and probed for ApoEr2 (Fig. 1*K*) or immunoprecipitated for ApoEr2 and probed for X11α (Fig. 1*L*). ApoEr2 constructs possessing exon 19, but not exon 18 alone, coprecipitated with X11α, consistent with a recent publication (22).

PDZ domain of X11α interacts with ApoEr2

To test which domain of X11α interacts with ApoEr2, we generated Flag-tagged X11α constructs containing fragments of X11α: PDZ domains (both PDZa and PDZb; construct 1), PTB domain only (construct 2), or the PTB and PDZ domains together (construct 3), along with full-length X11α (construct 4) (**Fig. 2*A***). To first determine whether the X11α PTB domain interacted with APP in our system, we cotransfected COS7 cells with full-length APP and X11α constructs 1, 2, and 4. Expected protein sizes were expressed from each construct, as determined by Western blots (Fig. 2*B*). Using the same cell lysate, we immunoprecipitated APP and probed for X11α. The constructs containing the X11α PTB domain coprecipitated with APP, but the X11α PDZ domain alone did not (Fig. 2*C*), consistent with previous findings (26).

We then asked which domain of X11α interacted with ApoEr2. Expected protein sizes were expressed from each construct, as determined by Western blots with anti-Flag (Fig. 2*D*). We cotransfected COS7 cells with full-length ApoEr2 and X11α deletion mutants (Fig. 2*A*). We then immunoprecipitated ApoEr2 with anti-HA antibody and probed with anti-Flag antibody for X11α. The X11α construct lacking the PDZ domain did not coprecipitate with ApoEr2 even after overexposure of the blots, but the constructs containing the PDZ domains did. We verified that total ApoEr2 levels were consistent across transfections (Fig. 2*E*). We also performed the reverse experiment, including the full-length X11α construct (construct 4); again, we observed that constructs containing the X11α PDZ domains coprecipitated with ApoEr2, but the construct containing the PTB domain alone did not (Fig. 2*F*). Thus, the interaction of X11α with ApoEr2 depended on the PDZ domains of X11α.

We then conducted yeast 2-hybrid analysis to independently determine which domain of X11 interacted with ApoEr2. For these experiments, we utilized the β-galactosidase reporter system and observed a colorimetric reaction in response to activation. We generated

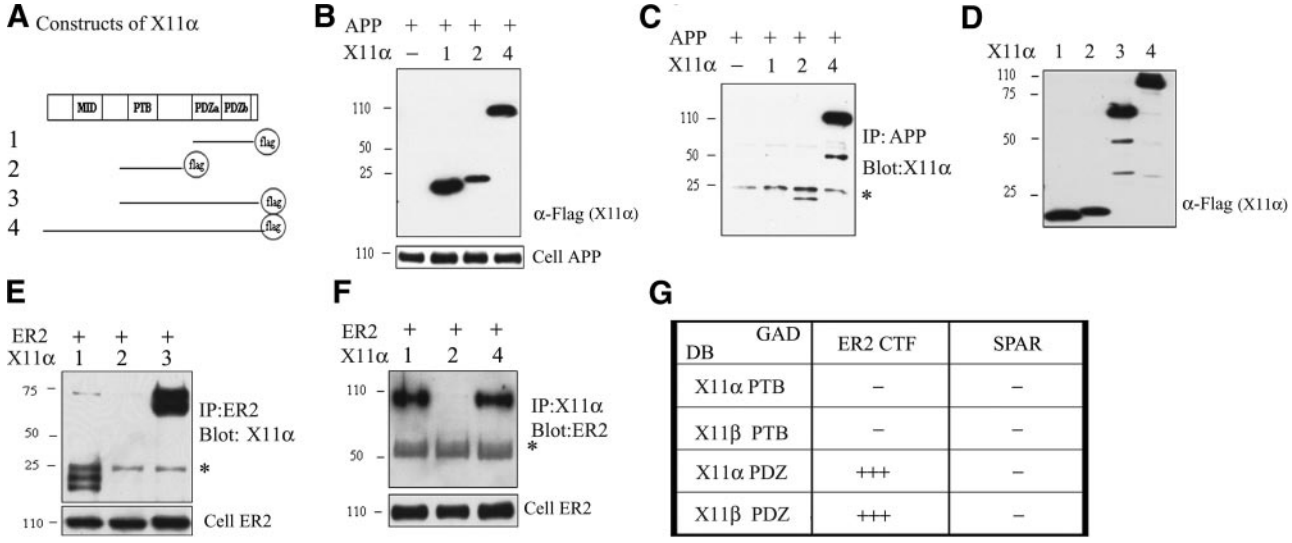

DB \ GAD	ER2 CTF	SPAR
X11α PTB	–	–
X11β PTB	–	–
X11α PDZ	+++	–
X11β PDZ	+++	–

Figure 2. ApoEr2 interacts with X11α PDZ domains. *A*) Constructs of X11α with C-terminal Flag tags containing PDZa and PDZb (construct 1), only PTB (construct 2), PTB and both PDZ domains (construct 3), and full-length X11α (construct 4). *B*) Lysates from COS7 cells transfected with different X11α deletion constructs were probed with anti-Flag to demonstrate protein expression. *C*) COS7 cells were transiently transfected with APP and X11α, as indicated. Cell lysates were immunoprecipitated with APP and probed with anti-Flag (n=2). *D*) COS7 cells were transfected with X11α as indicated and probed for anti-Flag to visualize X11α expression. *E, F*) COS7 cells were transfected with ApoEr2 and X11α as indicated. Cell lysates were immunoprecipitated with anti-HA and probed with anti-Flag (n=3) (*E*) or immunoprecipitated with anti-Flag and probed with anti-HA (*F*). Full-length X11α and PDZ domains of X11α interact with ApoEr2. Cell lysates were probed for HA to demonstrate ApoEr2 expression. *G*) ApoEr2 CTF fused to the GAL4 activation domain (GAD) interacts with the PDZ domains of X11α and X11β bound to the LexA DNA binding domain (DB), but the PTB domain of X11α or X11β did not. SPAR is used as a negative control (n=4). +++, 0–30 min β-gal detection time; –, no detectable β-gal signal after 12 h.

ApoEr2 CTF or SPAR (as a negative control) fused to the GAL4 activation domain, and PTB or PDZ fragments of X11α or X11β fused to the LexA DNA binding domain. We transformed these constructs into yeast, and within 15 min, there was detectable β-gal signal for ApoEr2 CTF with X11α PDZ or X11β PDZ domains (Fig. 2*G*). ApoEr2 CTF with the X11α or X11β PTB domains did not produce a β-galactosidase signal for up to 12 h (Fig. 2*G*). The negative control, SPAR, did not interact with any domain of X11α or X11β tested. Thus, the immunoprecipitation assays and yeast 2-hybrid assays demonstrate that the exon 19 region of ApoEr2 interacts with the PDZ domains of X11.

Reelin decreased coprecipitation of ApoEr2 and X11α in primary neurons

Reelin affects the trafficking and processing of both ApoEr2 and APP (7). To test whether extracellular ligands such as Reelin alter the interaction between ApoEr2 and X11α, we treated primary neuronal cells with control or Reelin-containing medium for 20 min. As controls, we immunoprecipitated neuronal lysates with anti-ApoEr2 and probed for ApoEr2 (**Fig. 3*A***), and immunoprecipitated with anti-X11α and probed for X11α (Fig. 3*B*), demonstrating consistent expression across conditions.

Next, we immunoprecipitated lysates from control or Reelin-treated neurons with anti-X11α or ApoEr2 and probed for ApoEr2 or X11α, respectively. Under control treatment, X11α and ApoEr2 coprecipitated. However, Reelin treatment decreased coprecipitation between X11α and ApoEr2 by 81 or 88% (Fig. 3*C*, *D*). These data suggest that Reelin may regulate the intracellular binding of ApoEr2 and X11α.

To test whether Reelin alters colocalization between ApoEr2 and X11α using an independent assay, we treated primary hippocampal neurons with control or Reelin-containing medium for 24 h. We immunostained primary neurons with antibodies against ApoEr2 and X11α and measured colocalization of puncta. Reelin decreased colocalization between ApoEr2 and X11α in neuronal processes compared to control by 22% ($P<0.05$, $n=12$) (Fig. 3*E*).

To determine whether Reelin also altered the interaction between APP and X11α, we treated primary neurons with control or Reelin-containing medium for 20 min. We immunoprecipitated neuronal lysates with anti-X11α or APP and probed for APP or X11α, respectively. Under control treatment, X11α and APP copre-

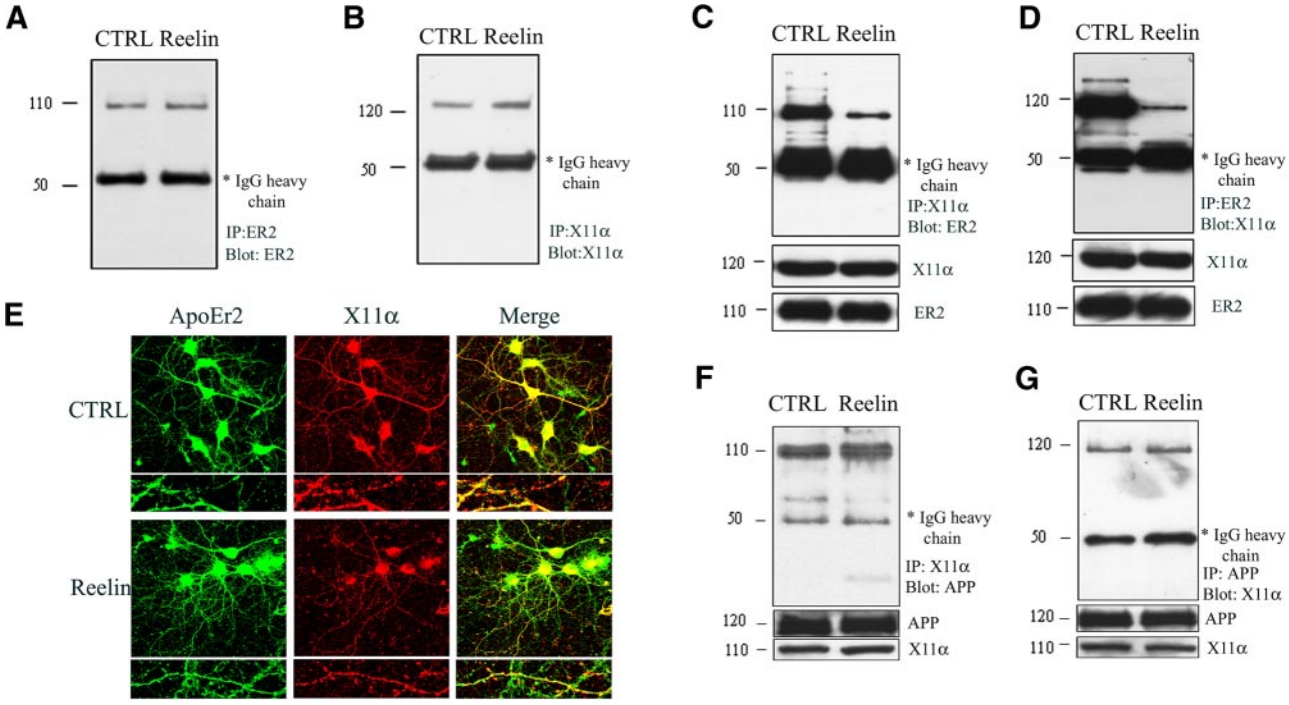

Figure 3. Reelin decreased coprecipitation of ApoEr2 and X11α in primary neurons. *A–D*) Primary neuronal proteins were treated with Reelin or control-conditioned medium for 24 h. Primary neurons were immunoprecipitated with ApoEr2 and probed with ApoEr2 (*A*) or immunoprecipitated with X11α and probed with X11α to demonstrate expression (*B*). Primary neurons were immunoprecipitated with X11α and probed with ApoEr2 (*C*) or immunoprecipitated with ApoEr2 and probed with X11α (*D*). Reelin decreased coprecipitation of ApoEr2 and X11α by 81 and 88%, respectively ($n=3$; $P<0.01$). Immunoblot of cell lysates showed similar levels of ApoEr2 and X11α. *E*) Primary hippocampal neurons (DIV12) were treated with control or Reelin-containing medium for 24 h, immunostained for ApoEr2 (left panel) and anti-X11α (middle panel), and observed under a confocal laser-scanning microscope (×63). Right panel shows colocalization of ApoEr2 (green) and X11α (red) ($n=12$). *F, G*) Primary neurons were treated with Reelin or control-conditioned medium and immunoprecipitated with X11α and probed with APP (*F*) or immunoprecipitated with APP and probed with X11α (*G*). Reelin did not affect the coprecipitation of APP and X11α ($n=3$).

cipitated, and Reelin did not affect the coprecipitation between X11α and APP (Fig. 3*F, G*). These data suggest that Reelin specifically affects the interaction between X11α and ApoEr2 but not between X11α and APP.

X11α promotes Fyn-mediated ApoEr2 phosphorylation, and Reelin reverses this effect

Tyrosine phosphorylation of the intracellular domain of membrane proteins is known to affect their interactions with specific adaptor proteins as well as their trafficking. We and others have shown that Fyn tyrosine kinase phosphorylates APP and ApoEr2 (27). To test whether X11α alters the tyrosine phosphorylation of ApoEr2 and whether it can specifically alter Fyn-mediated tyrosine phosphorylation of ApoEr2, we transfected COS7 cells with indicated constructs. We then immunoprecipitated cell lysates for phosphotyrosine and Western blotted for ApoEr2 (**Fig. 4*A***). Cells triply transfected with ApoEr2, X11α, and Fyn had higher levels of phospho-ApoEr2 compared to X11α or Fyn alone, suggesting that X11α modulates tyrosine phosphorylation of ApoEr2 by Fyn. Interestingly, phospho-ApoEr2 levels were increased in the presence of Fyn with Reelin treatment, but phospho-ApoEr2 levels were reduced in the presence of both X11α and Fyn with Reelin treatment. Thus, X11α promotes Fyn-mediated phosphorylation of ApoEr2, but Reelin prevents this effect. Quantification of data showed a significant 186% increase in phospho-ApoEr2 in the presence of both X11α and Fyn compared to X11α alone and a 109% increase compared to Fyn alone (normalized to total ApoEr2) (Fig. 4*B*). Reelin treatment together with overexpression of Fyn increased phospho-ApoEr2 levels by 214% compared to control, but in the added presence of X11α, phospho-ApoEr2 was decreased by 47%.

Fyn increases association between ApoEr2 and X11α, and Reelin reverses this effect

To test whether the Fyn-mediated increase in ApoEr2 phosphorylation is correlated with a greater interaction between ApoEr2 and X11α, COS7 cells were transfected with ApoEr2, X11α, and vector (Fig. 4*C*, lane 1) or ApoEr2, X11α, and Fyn (Fig. 4*C*, lane 2). Coexpression of Fyn increased the association between ApoEr2 and X11α by 153% ($P<0.05$). Next, we tested whether Reelin modulated the ApoEr2-X11α interaction in the presence of Fyn. For this experiment, we triply transfected cells with ApoEr2, X11α, and Fyn and treated with control (Fig. 4*C*, lane 2) or Reelin (Fig. 4*C*, lane 3) for 20 min. Reelin treatment decreased the Fyn-induced increase in interaction between ApoEr2 and X11α.

X11α increases cell-surface ApoEr2 in MCF 10A cells

Adaptor protein interactions with APP are known to influence a variety of downstream effects, including cell migration (15). ApoEr2 is also known to affect cell migration (3, 28), so we analyzed cell movement with a wound-healing assay in MCF 10A cells. First, we tested endogenous levels of APP, ApoEr2, and cytoplasmic adaptor proteins in MCF 10A cells compared to COS7 cells, where our initial studies were performed (Figs. 1–4). We found a robust expression of the adaptor proteins Dab1, X11α, and FE65 in MCF 10A cells, while COS7 cells had no detectable Dab1 or X11α but greater expression of FE65. MCF 10A cells did not express APP or ApoEr2, while COS7 cells had some detectable expression following prolonged exposure (**Fig. 5*A***).

Next, we examined whether Reelin treatment altered the interaction between ApoEr2 and X11α in MCF 10A

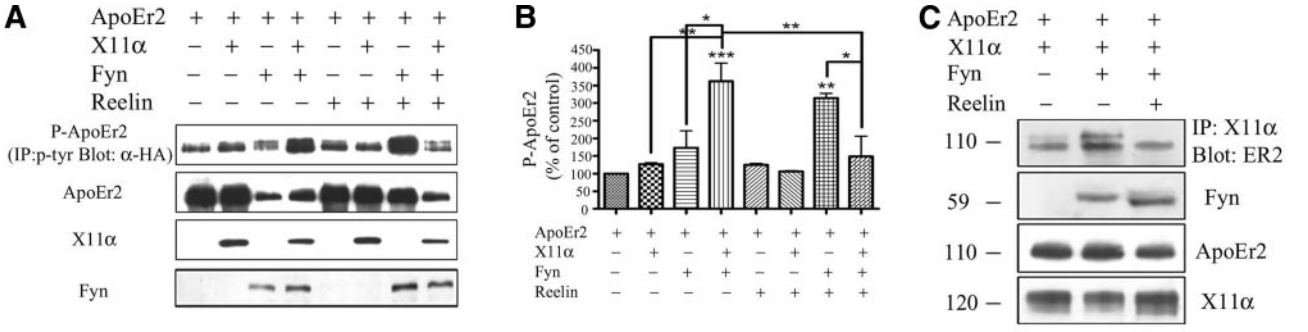

Figure 4. Reelin decreases Fyn- and X11α-mediated tyrosine phosphorylation of ApoEr2 and decreases Fyn-mediated interaction between ApoEr2 and X11α. *A*) COS7 cells were transfected with ApoEr2 and vector, X11α, Fyn, or both X11α and Fyn for 24 h, and treated with control or Reelin-conditioned medium for 20 min. Cell lysates were immunoprecipitated for phosphotyrosine and Western blotted for ApoEr2 (α-HA) to detect tyrosine phosphorylated ApoEr2. *B*) Quantification of data shows that ApoEr2, Fyn, and X11α increased phospho-ApoEr2 levels by 186% (lane 4) compared to ApoEr2 and X11α ($P<0.01$) (lane 2) and by 109% compared to ApoEr2 and Fyn ($P<0.05$) (lane 3). Reelin treatment of ApoEr2 and Fyn transfected cells increased phospho-ApoEr2 by 214% ($P<0.01$) (lane 7), and Reelin treatment of cells triply transfected with X11α, ApoEr2, and Fyn decreased phospho-ApoEr2 by 47% ($P<0.05$) (lane 8). *C)* COS7 cells were transfected with ApoEr2, X11α, and vector (lane 1) or Fyn (lane 2), and treated with control medium, or transfected with ApoEr2, X11α, and Fyn and treated with Reelin for 20 min (lane 3). Lysates were immunoprecipitated with anti-Flag for X11α and Western blotted with anti-HA for ApoEr2 (top panel). Fyn increased the interaction between ApoEr2 and X11α by 153% (lane 2, $P<0.05$), and Reelin treatment reversed this effect (by 42%; lane 3 *vs.* lane 2). Bottom panels show consistent expression patterns.

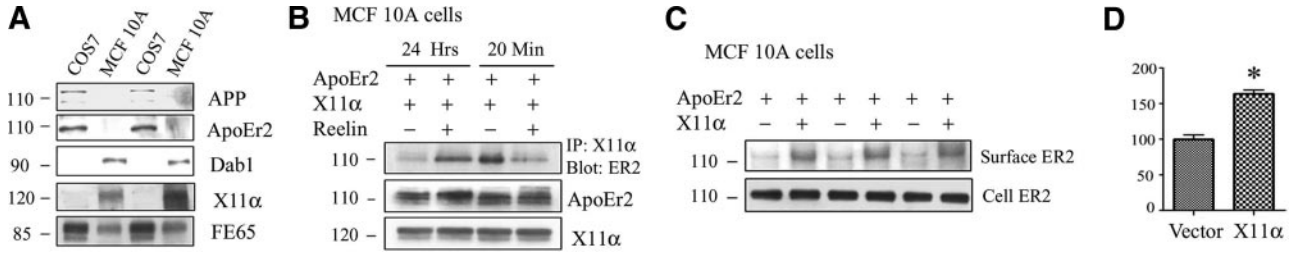

Figure 5. Reelin alters interaction between X11α and ApoEr2, and X11α increases cell-surface ApoEr2 in MCF 10A cells. *A*) Cell lysates from COS7 and MCF 10A cells were Western blotted for APP, ApoEr2, Dab1, X11α, and FE65 to demonstrate expression. COS7 cells expressed detectable levels of APP and ApoEr2, but no expression of Dab1 and X11α with a high level of FE65. MCF 10A cells did not express APP or ApoEr2 but did express Dab1, X11α, and FE65. *B*) MCF 10A cells were cotransfected with ApoEr2 and X11α and treated with either control (lanes 1 and 3) or Reelin (lanes 2 and 4) for 24 h (lanes 1 and 2) or 20 min (lanes 3 and 4). Cell lysates were immunoprecipitated with anti-Flag for X11α and Western blotted for ApoEr2. Reelin decreased coprecipitation between ApoEr2 and X11α at 20 min (41%), but increased coprecipitation at 24 h (223%). *C*) MCF 10A cells were cotransfected with GFP-ApoEr2 and either vector (lanes 1, 3, and 5) or X11α (lanes 2, 4, and 6). Cell-surface proteins were biotin labeled, isolated with avidin beads, and immunoblotted with GFP for ApoEr2. Cell lysates showed similar levels of total ApoEr2. *D*) Quantification of data in *C* showed that full-length X11α increased surface levels of ApoEr2 by 64% ($n=3$) $^*P < 0.05$.

cells. For this experiment, we transfected MCF 10A cells with ApoEr2 and X11α and treated with control or Reelin for 20 min or 24 h. We immunoprecipitated cell lysates for X11α and Western blotted for ApoEr2 and found that Reelin decreased the interaction between X11α and ApoEr2 after 20 min (by 41%, Fig. 5*B*, right lanes), consistent with previous results in primary neurons (Fig. 3*C*, *D*). However, Reelin increased the interaction between ApoEr2 and X11α after 24 h (by 223%, Fig. 5*B*; left lanes), suggesting a time-dependent effect of Reelin on the association between ApoEr2 and X11α. Expression levels of X11α and ApoEr2 were consistent across conditions (Fig. 5*B*, bottom panels). These results suggest that Reelin can alter the intracellular association between ApoEr2 and X11α in MCF 10A cells in a time-dependent manner.

To determine whether X11α alters the trafficking of ApoEr2 in MCF 10A cells, we cotransfected cells with ApoEr2 and vector or X11α. Levels of cell-surface ApoEr2 were increased by full-length X11α, while levels of total ApoEr2 were unchanged (Fig. 5*C*). Quantification of data demonstrated a 64% increase in cell-surface ApoEr2 by X11α (Fig. 5*D*).

ApoEr2 accelerates cell migration in a wound-healing assay

Previous studies using a wound-healing assay have shown that APP plays an important role in cell movement (15). ApoEr2 is also involved in neuronal migration (28, 29); however, whether it directly facilitates cell movement in a wound-healing assay is unknown. To determine whether ApoEr2 or X11α had an effect on cell movement, we transfected epithelial MCF 10A cells with indicated constructs, and gap width was measured at 0, 8, 16, and 24 h following transfection (**Fig. 6*A***). APP significantly decreased gap width at all time points, consistent with previous findings (15). We found that ApoEr2 also markedly decreased gap width, and gap width between APP- and ApoEr2-expressing cells was not significantly different. Gap width following transfection with X11α alone was not significantly different compared to control at 8 h and experienced only a mild reduction at 16 and 24 h (Fig. 6*B*). Cotransfection of X11α with either APP or ApoEr2 did not affect gap width compared to that of APP or ApoEr2 alone. Thus, APP and ApoEr2 both increased cell movement, but X11α did not alter these effects.

We then determined the rate of migration of individual cells in separate experiments and similarly found that APP and ApoEr2 significantly increased cell velocity along the wound edge, by 54 and 87%, respectively (Fig. 6*C*). ApoEr2 accelerated cell motility to a greater extent than APP. X11α alone had no affect on cell velocity. Cotransfection of ApoEr2 and X11α increased cell velocity by 13% compared to ApoEr2 alone (Fig. 6*C*), but cotransfection of APP and X11α did not significantly alter velocity compared to APP alone. These data show that APP, and ApoEr2 to an even greater extent, dramatically decreases gap width and increases cell velocity, and that X11α had small or no effects on cell motility along the wound edge.

Knockdown of endogenous X11α eliminates the effect of ApoEr2 on cell motility

To further test the effect of the interaction between ApoEr2 and X11α on cell motility, we performed a similar wound-healing experiment using a construct of ApoEr2 lacking exon 19 (the interaction site for X11α) and using siRNA against endogenous X11α (**Fig. 7**). We first determined the optimal concentration for knockdown of X11α in MCF 10A cells by transfecting with 50, 100, or 200 nM of X11α siRNA for 24 h, which resulted in efficient knockdown of X11α at 100 and 200 nM by >88% (Fig. 7*A*). We also monitored cell toxicity and did not observe toxicity at any concentration (data not shown). Next, we conducted a wound-healing assay and measured gap width at 0, 8, 16, and 24 h following wounding (Fig. 7*B*, *C*, *E*). ApoEr2 decreased gap width by 24 h compared to control, as previously shown (Fig. 6*B*). However, ApoEr2 lacking exon 19 had a signifi-

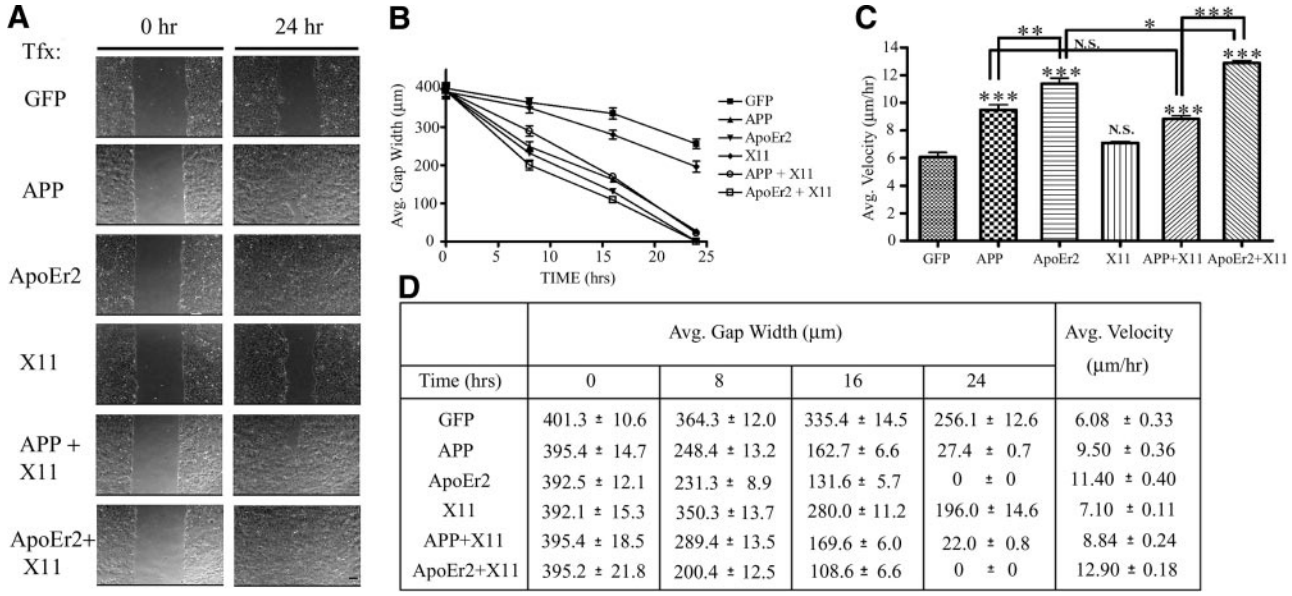

D

	Avg. Gap Width (μm)				Avg. Velocity (μm/hr)
Time (hrs)	0	8	16	24	
GFP	401.3 ± 10.6	364.3 ± 12.0	335.4 ± 14.5	256.1 ± 12.6	6.08 ± 0.33
APP	395.4 ± 14.7	248.4 ± 13.2	162.7 ± 6.6	27.4 ± 0.7	9.50 ± 0.36
ApoEr2	392.5 ± 12.1	231.3 ± 8.9	131.6 ± 5.7	0 ± 0	11.40 ± 0.40
X11	392.1 ± 15.3	350.3 ± 13.7	280.0 ± 11.2	196.0 ± 14.6	7.10 ± 0.11
APP+X11	395.4 ± 18.5	289.4 ± 13.5	169.6 ± 6.0	22.0 ± 0.8	8.84 ± 0.24
ApoEr2+X11	395.2 ± 21.8	200.4 ± 12.5	108.6 ± 6.6	0 ± 0	12.90 ± 0.18

Figure 6. ApoEr2 increases cell migration in a wound-healing assay. *A*) MCF 10A cells were transfected with constructs indicated at left. A single monolayer of cells was scraped with a pipette tip and immediately imaged (left panels). Right panels show representative images of the wound gap 24 h later. Scale bars = 75 μm. *B*) Closure of the wound gap was measured at 0, 8, 16, and 24 h by average gap width. By 24 h, X11α had a slightly lower gap width compared to GFP control (23%; $P<0.01$); however, this decrease was significantly different from APP (89%; $P<0.001$), APP + X11α (91%; $P<0.001$), ApoEr2, and ApoEr2 + X11α (100%; $P<0.001$) ($n=3$). *C*) Average velocity of individual cells along the wound edge was measured over a 24-h period. Cotransfection of APP or ApoEr2 significantly increased average velocity of cells compared to control (by 54 and 87%) or X11α alone, and cotransfection of ApoEr2 with X11α resulted in a significant increase compared to ApoEr2 alone (by 13%) ($n=4$). $*P < 0.05$, $**P < 0.01$, $***P < 0.001$. *D*) Table of values showing quantification for *B* and *C*.

cantly greater gap width by 24 h compared to full-length ApoEr2. In addition, ApoEr2 and X11α decreased gap width compared to control at 24 h; however, ApoEr2 and X11α siRNA increased gap width compared to ApoEr2 and X11α or ApoEr2 alone.

We next determined whether the interaction between ApoEr2 and X11α affected cell velocity in an independent experiment (Fig. 7*D*, *E*). ApoEr2 lacking exon 19 decreased cell velocity compared to full-length ApoEr2 (28% decrease; $P<0.001$). X11α siRNA with ApoEr2 decreased cell velocity compared to ApoEr2 and X11α (35% decrease) or ApoEr2 alone (27% decrease), implying a role for endogenous X11α in facilitating the effects of ApoEr2 on cell motility. These data suggest that exon 19 of ApoEr2, which interacts with X11α, is important for its effects on wound healing, and that endogenous X11α plays a role in ApoEr2-mediated cell motility.

Reelin increases the effect of ApoEr2 and X11α on cell motility in a wound-healing assay

Reelin is a ligand for both APP and ApoEr2 and is known to be essential for proper neuronal migration during development. To test whether Reelin could modulate the effect of APP or ApoEr2 on cell motility, we performed a similar, independent, wound-healing assay and transfected MCF 10A cells treated with control or Reelin-conditioned medium (**Fig. 8*A***). Consistent with previous findings (Fig. 6*B*), X11α alone did not decrease gap width compared to control by 24 h, but APP and ApoEr2 did (Fig. 8*B*). Reelin treatment alone did not decrease gap width, consistent with previously published studies (30). X11α together with Reelin treatment also did not decrease gap width at 8 or 16 h and only slightly decreased gap width by 24 h. We found that Reelin treatment of APP-transfected cells did not significantly decrease gap width any further than APP alone; however, Reelin treatment of ApoEr2 transfected cells did significantly decrease gap width at 8 and 16 h compared to ApoEr2 alone. Furthermore, gap width was decreased in cells transfected with ApoEr2 compared to APP at 16 and 24 h, and Reelin treatment decreased gap width in ApoEr2 compared to APP-transfected cells both in the absence and presence of X11α. There was no gap observed by 24 h for all ApoEr2-transfected conditions, suggesting a major role for ApoEr2 in cell migration in a wound-healing assay.

We additionally measured individual cell velocities along the wound edge and found that Reelin, X11α, or Reelin and X11α together did not increase average cell velocity, but all cells transfected with APP or ApoEr2 did have significant increases in cell velocity (Fig. 8*C*). Treatment with Reelin or cotransfection with X11α did not further increase the effect of APP on cell velocity. Reelin treatment and transfection with X11α, however, significantly increased the effect of ApoEr2 on cell velocity, by 20 and 15%, respectively (Fig. 8*C*). Cotransfection of ApoEr2 and X11α together with Reelin treatment further increased cell velocity compared to

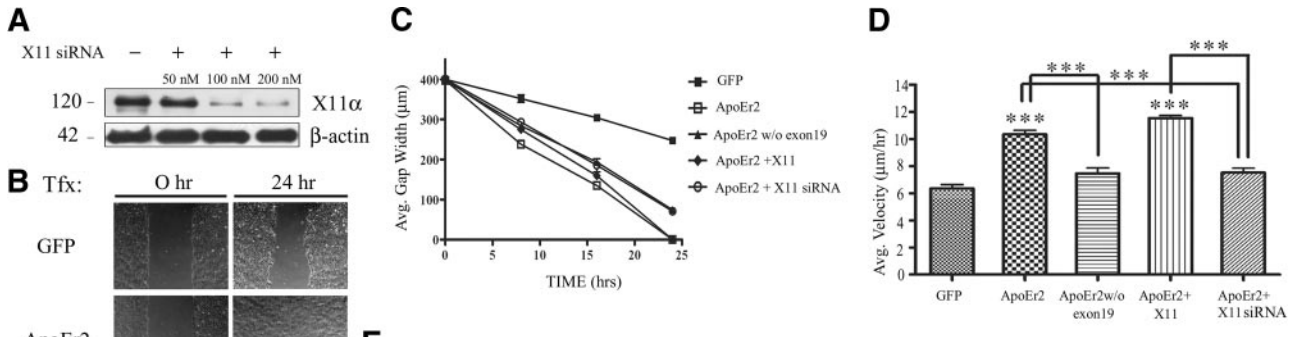

E

	Avg. Gap Width (μm)				Avg. Velocity (μm/hr)
Time (hrs)	0	8	16	24	
GFP	400.1 ± 1.9	352.1 ± 9.3	304.2 ± 7.2	247.4 ± 4.0	6.35 ± 0.29
ApoEr2	397.7 ± 3.3	238.1 ± 9.2	135.1 ± 4.5	0 ± 0	10.35 ± 0.3
ApoEr2w/oexon19	397 ± 4	284.1 ± 6.1	193.5 ± 3.4	74.4 ± 7.8	7.47 ± 0.39
ApoEr2+X11	399.2 ± 1.9	274.5 ± 5.0	159.7 ± 6.0	0 ± 0	11.55 ± 0.18
ApoEr2+ X11 si RNA	401.1 ± 6.3	293.3 ± 4.7	185.8 ± 16.5	71.1 ± 6.4	7.52 ± 0.31

Figure 7. Interaction between ApoEr2 and X11α promotes cell migration in a wound-healing assay. *A*) MCF 10A cells were transfected with 50, 100, or 200 nM of siRNA against X11α for 24 h. X11α siRNA resulted in >88% knockdown of X11α at 100 and 200 nM. *B*) MCF 10A cells were transfected with constructs indicated at left. A single monolayer of cells was scraped with a pipette tip and immediately imaged (left panels). Right panels show representative images of the wound gap 24 h later. *C*) Closure of the wound gap was measured at 0, 8, 16, and 24 h by average gap width. By 24 h, ApoEr2 lacking exon 19 increased gap width compared to full-length ApoEr2 ($P<0.001$). ApoEr2 with X11α siRNA increased gap width compared to cotransfection of ApoEr2 with X11α ($P<0.001$) or ApoEr2 alone ($P<0.001$). *D*) Average velocity of individual cells along the wound edge was measured over a 24-h period. ApoEr2 alone or ApoEr2 + X11α significantly increased average velocity of cells compared to control (by 63 and 82%; $P<0.001$). ApoEr2 lacking exon 19 decreased cell velocity compared to full-length ApoEr2 (by 28%; $P<0.001$) and ApoEr2 + X11α siRNA resulted in a significant decrease compared to ApoEr2 + X11α (by 35%; $P<0.001$) or ApoEr2 alone (by 27%; $P<0.001$) ($n=4$). ***$P < 0.001$. *E*) Table of values showing quantification for *C* and *D*.

ApoEr2 and X11α alone (Fig. 8*C*), but not compared to ApoEr2 and Reelin treatment alone, suggesting that Reelin may modulate the effect of X11α and ApoEr2, but X11α does not modulate the effect of Reelin and ApoEr2 on cell velocity. A table of values for average gap width and average velocity is shown in Fig. 8*D*. These data show that Reelin treatment further enhances the effect of ApoEr2, and the combined effect of ApoEr2 and X11α, on cell migration along the wound edge.

DISCUSSION

In this study, we identified an interaction between the intracellular domain of ApoEr2 (exon 19) and the PDZ domains of X11α and X11β, which resulted in increased cell-surface ApoEr2 and increased tyrosine phosphorylation of ApoEr2. In addition, we demonstrated that the interaction between ApoEr2 and X11α can be modulated by the addition of extracellular ligands such as Reelin in a time-dependent manner, where Reelin decreased the association between ApoEr2 and X11α after 20 min but increased association after 24 h of treatment. We show a novel role for ApoEr2 in cell movement using a wound-healing assay in MCF 10A cells, which was facilitated by X11α and Reelin, implying an important role for adaptor proteins and extracellular ligands in mediating the functional effects of membrane receptors.

Adaptor proteins containing PTB domains are known to interact with APP and ApoEr2 and may compete for binding. For example, X11α and Dab1 both bind the NPTY sequence of APP and exert opposing effects on APP trafficking and processing (26, 31, 32). In addition, X11β was also shown to compete with FE65 for binding to APP (31). Similarly, our studies have shown that Dab1 and FE65 interact with the NPVY sequence of ApoEr2 (7, 8). Interestingly, we and others found that the ^{899}YDRPLW^{904} sequence of ApoEr2 is important for binding to X11α, suggesting that X11α may not compete with Dab1 and FE65 for binding to ApoEr2 (22).

Competition can also exist between receptors for the same adaptor protein. For example, both ApoEr2 and APP interact with the PTB domain of Dab1 (7). Conversely, the first PTB domain of FE65 interacts with ApoEr2, while the second PTB domain of FE65 interacts with APP, suggesting that FE65 may bind to APP and ApoEr2 simultaneously (8). He *et al.* (22) previously suggested a model where APP and ApoEr2 compete for binding to X11α, based on data which showed that the PTB domain of X11α interacted with ApoEr2. However, it is possible that because X11α does not

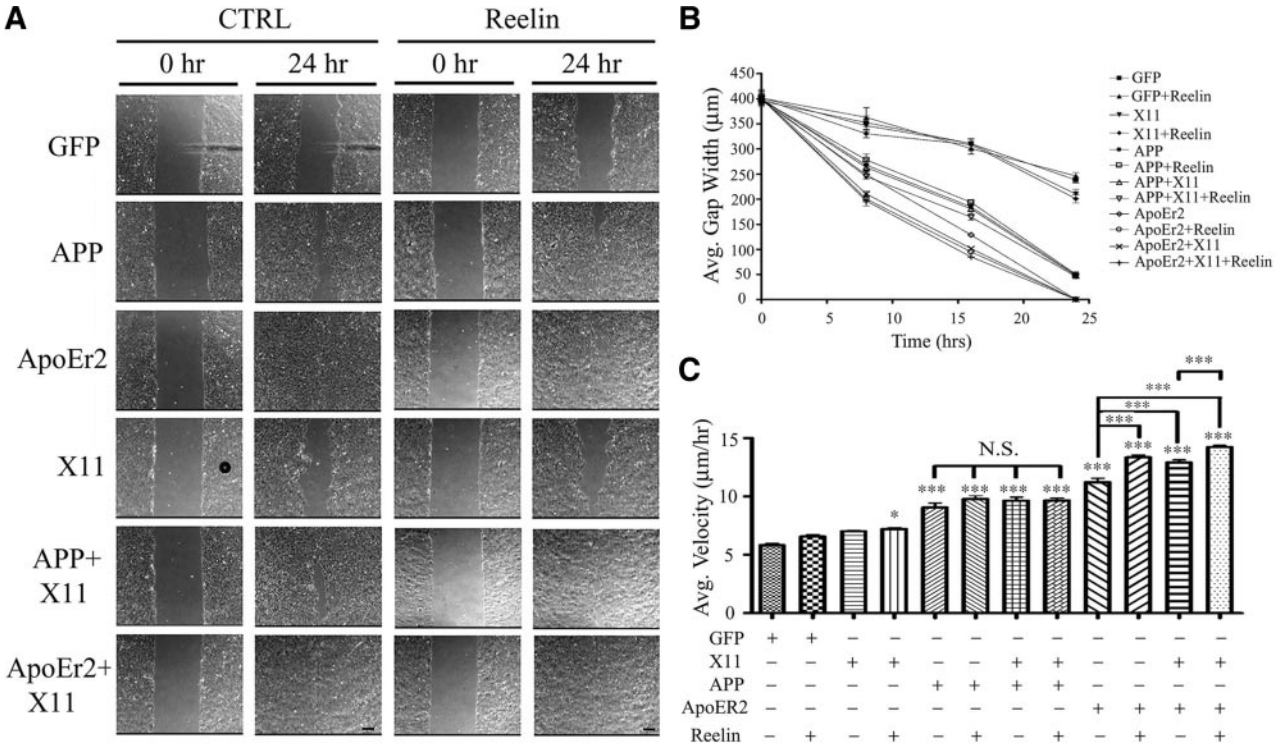

D

	Avg. Gap Width (μm)				Avg. Velocity (μm/hr)
Time (hrs)	0	8	16	24	
GFP	395.2 ± 8.4	352.5 ± 13.3	310.5 ± 10.2	238.1 ± 5.5	5.83 ± 0.15
GFP+Reelin	401.4 ± 15.3	363.1 ± 19.2	300.9 ± 11.1	246.3 ± 6.9	6.85 ± 0.14
X11	402.1 ± 10.2	346.5 ± 11.6	311.0 ± 8.5	210.3 ± 9.5	7.03 ± 0.06
X11+Reelin	400.2 ± 8.2	330.2 ± 8.0	308.6 ± 11.7	200.8 ± 8.4	7.21 ± 0.12
APP	398.6 ± 7.8	267.9 ± 11.7	184.5 ± 4.2	49.0 ± 1.2	9.08 ± 0.36
APP+Reelin	397.4 ± 10.0	278.4 ± 11.7	193.6 ± 5.4	50.0 ± 1.5	9.78 ± 0.32
APP+X11	400.1 ± 10.7	263.2 ± 8.3	180.5 ± 11.6	47.0 ± 0.5	9.65 ± 0.30
APP+X11+Reelin	400.3 ± 10.0	245.3 ± 3.3	164.4 ± 5.8	46.0 ± 1.2	9.67 ± 0.19
ApoEr2	396.9 ± 9.5	249.0 ± 8.5	128.5 ± 0.8	0 ± 0	11.23 ± 0.35
ApoEr2+Reelin	400.7 ± 5.9	200.5 ± 6.6	95.0 ± 3.3	0 ± 0	13.35 ± 0.21
ApoEr2+X11	401.4 ± 17.4	210.5 ± 5.9	101.5 ± 1.8	0 ± 0	12.93 ± 0.21
ApoEr2+X11+Reelin	400.5 ± 14.0	196.4 ± 10.0	85.0 ± 2.4	0 ± 0	14.23 ± 0.15

Figure 8. Reelin increases the effects of X11α and ApoEr2 in a wound-healing assay. *A*) MCF 10A cells were transfected with constructs indicated at left and treated with control (left panels) or Reelin-conditioned medium (right panels) for 24 h. Representative images of the wound gap at 0 h (left) and 24 h (right) are shown. Scale bars = 75 μm. *B*) Average gap width was measured at 0, 8, 16, and 24 h following control or Reelin treatment. By 24 h, X11α or Reelin alone did not decrease gap width compared to GFP. X11α + Reelin slightly decreased gap width (16%; $P<0.05$); however, this decrease was significantly different from that of APP (79%), APP + Reelin (79%), APP + X11α (80%), APP + X11α + Reelin (81%), and all conditions, including ApoEr2 (100%) ($P<0.001$ for all). ApoEr2 further decreased gap width compared to APP alone ($P<0.001$), in the presence of X11α ($P<0.01$), with Reelin treatment ($P<0.001$), and in the presence of X11α + Reelin treatment ($P<0.01$). *C*) Average velocity of individual cells along the wound edge was measured over a 24-h period. Cotransfection of APP or ApoEr2 significantly increased average velocity of cells compared to control (56 and 93%) or X11α alone, and cotransfection of ApoEr2 with X11α resulted in a significant increase compared to ApoEr2 alone (122%). Reelin alone increased cell velocity in ApoEr2-transfected cells (19%) and also significantly increased cell velocity compared to control treatment of ApoEr2 + X11α-transfected cells (10%) ($n=4$). *$P < 0.05$, ***$P < 0.001$. *D*) Table of values showing quantification for *B* and *C*.

interact with the ApoEr2 NPXY domain, which binds PTB domain-containing adaptor proteins, it is not the PTB domain of X11α that interacts with ApoEr2, but rather the PDZ domain, as we demonstrate here (Fig. 2*E–G*). These results suggest that not only does X11α not compete with other adaptor proteins for binding to ApoEr2 but that X11α also does not spur competition between APP and ApoEr2 by binding at distinct domains on their cytoplasmic tails.

X11α has been shown to affect the overall metabo-

lism of APP through modulation of secretory and endocytic trafficking (33–35). We show a direct effect of X11α on increasing cell-surface levels of ApoEr2 in MCF 10A cells (Fig. 5*C*). Phosphorylation of the C-terminal of membrane receptors is one way in which adaptor proteins can regulate trafficking of these receptors (36). We found that X11α can increase tyrosine phosphorylation of ApoEr2 by Fyn, suggesting a possible mechanism by which X11α mediates the trafficking of ApoEr2.

APP and ApoEr2 are known to play important roles in neuronal migration (9, 30). APP has been shown to increase cell motility in wound-healing assays, an effect further enhanced by its interaction with FE65 (15). In our studies, we similarly saw an effect of APP on wound healing in MCF 10A cells, and additionally found a novel role for ApoEr2 in wound healing. We then tested whether interaction with X11α could alter the effect of APP or ApoEr2 on wound healing similar to FE65, as X11α is known to interact with cell-adhesion molecules in *Drosophila* (37) and also with kalirin-7, a Rho-GEF that regulates dendritic morphogenesis (38). By interacting with an array of cell-adhesion and cytoskeletal proteins, as well as ApoEr2, X11α may serve as a link to further facilitate cell movement. Our own studies showed that X11α increases cell-surface ApoEr2 in MCF 10A cells, providing a possible mechanism by which X11α can promote ApoEr2-mediated cell movement. Interestingly, X11α increased the effect of ApoEr2, but not APP, on wound healing in MCF 10A cells, suggesting a specific effect of X11α on ApoEr2 (Fig. 6). We further examined whether ApoEr2 ligands, such as Reelin, could alter the effects of APP or ApoEr2 on wound healing, and found that Reelin increased the effect of ApoEr2, but not APP, on cell motility, consistent with previous studies that implicate a role for ApoEr2-mediated Reelin signaling in cytoskeletal reorganization during neuronal migration (39). Notably, Reelin alone did not affect cell movement, as MCF 10A cells do not express ApoEr2 endogenously, suggesting that the presence of membrane receptors is necessary for Reelin to exert its effect. Interestingly, Reelin further increased the effect of ApoEr2 and X11α on cell movement, implying an additive effect of Reelin and X11α on ApoEr2-mediated cell movement.

CONCLUSIONS

Our present study contributes to growing evidence highlighting the significance of extracellular ligands and intracellular adaptor proteins in modulating the effects of membrane receptors. We established a role for X11α in regulating the phosphorylation and trafficking of ApoEr2, as well as ApoEr2-mediated cell movement, and these processes can be further modulated by Reelin. It is important to note that although APP and ApoEr2 may share common ligands, such as Reelin and X11α, the functional consequences of these interactions can differ significantly. We present novel roles for ApoEr2, X11α, and Reelin in modulating wound healing. However, further studies are needed to dissect the complex interactions that underlie ApoEr2- and Reelin-mediated cell movement. FJ

This work was supported by U.S. National Institutes of Health grants AG032330 (H.S.H.), AG030060 (G.W.R.), AG026478 (R.S.T.), and AG014473 (G.W.R.). We thank Dr. Christopher Miller and Dr. Declan McLoughlin (King's College London, London, UK) for X11 plasmid DNA, Dr. Joachim Herz (University of Texas Southwestern Medical Center, Dallas, TX, USA) for ApoEr2 (without exon19) plasmid DNA, and Dr. Andre Goffinet (Catholic University of Leuven, Brussels, Belgium) and Dr. Suzanne Guenette (Massachusetts General Hospital, Charlestown, MA, USA) for Dab1 and FE65 antibodies, respectively. We also thank Ji-yun Lee for her generous contribution toward the yeast 2-hybrid experiments.

REFERENCES

1. Selkoe, D. J. (2001) Alzheimer's disease: genes, proteins, and therapy. *Physiol. Rev.* **81,** 741–766
2. Corder, E. H., Saunders, A. M., Strittmatter, W. J., Schmechel, D. E., Gaskell, P. C., Small, G. W., Roses, A. D., Haines, J. L., and Pericak-Vance, M. A. (1993) Gene dose of apolipoprotein E type 4 allele and the risk of Alzheimer's disease in late onset families. *Science* **261,** 921–923
3. Herz, J., and Beffert, U. (2000) Apolipoprotein E receptors: linking brain development and Alzheimer's disease. *Nat. Rev. Neurosci.* **1,** 51–58
4. Herz, J., and Chen, Y. (2006) Reelin, lipoprotein receptors and synaptic plasticity. *Nat. Rev. Neurosci.* **7,** 850–859
5. Guenette, S. Y., Chen, J., Jondro, P. D., and Tanzi, R. E. (1996) Association of a novel human FE65-like protein with the cytoplasmic domain of the beta-amyloid precursor protein. *Proc. Natl. Acad. Sci. U. S. A.* **93,** 10832–10837
6. Gotthardt, M., Trommsdorff, M., Nevitt, M. F., Shelton, J., Richardson, J. A., Stockinger, W., Nimpf, J., and Herz, J. (2000) Interactions of the low density lipoprotein receptor gene family with cytosolic adaptor and scaffold proteins suggest diverse biological functions in cellular communication and signal transduction. *J. Biol. Chem.* **275,** 25616–25624
7. Hoe, H. S., Tran, T. S., Matsuoka, Y., Howell, B. W., and Rebeck, G. W. (2006) Dab1 and Reelin effects on APP and ApoEr2 trafficking and processing. *J. Biol. Chem.* **281,** 35176–35185
8. Hoe, H. S., Magill, L. A., Fu, Z., Vicini, S., and Rebeck, G. W. (2006) FE65 interaction with the apoE receptor ApoEr2. *J. Biol. Chem.* **281,** 24521–24530
9. Young-Pearse, T. L., Bai, J., Chang, R., Zheng, J. B., LoTurco, J. J., and Selkoe, D. J. (2007) A critical function for beta-amyloid precursor protein in neuronal migration revealed by in utero RNA interference. *J. Neurosci.* **27,** 14459–14469
10. Pramatarova, A., Chen, K., and Howell, B. W. (2008) A genetic interaction between the APP and Dab1 genes influences brain development. *Mol. Cell. Neurosci.* **37,** 178–186
11. Dulabon, L., Olson, E. C., Taglienti, M. G., Eisenhuth, S., McGrath, B., Walsh, C. A., Kreidberg, J. A., and Anton, E. S. (2000) Reelin binds α3β1 integrin and inhibits neuronal migration. *Neuron* **27,** 33–44
12. Bacskai, B. J., Xia, M. Q., Strickland, D. K., Rebeck, G. W., and Hyman, B. T. (2000) The endocytic receptor protein LRP also mediates neuronal calcium signaling via *N*-methyl-D-aspartate receptors. *Proc. Natl. Acad. Sci. U. S. A.* **97,** 11551–11556
13. Beffert, U., Weeber, E. J., Durudas, A., Qiu, S., Masiulis, I., Sweatt, J. D., Li, W. P., Adelmann, G., Frotscher, M., Hammer, R. E., and Herz, J. (2005) Modulation of synaptic plasticity and memory by Reelin involves differential splicing of the lipoprotein receptor Apoer2. *Neuron* **47,** 567–579
14. Chai, X., Forster, E., Zhao, S., Bock, H. H., and Frotscher, M. (2009) Reelin stabilizes the actin cytoskeleton of neuronal

processes by inducing n-cofilin phosphorylation at serine3. *J. Neurosci.* **29,** 288–299
15. Sabo, S. L., Ikin, A. F., Buxbaum, J. D., and Greengard, P. (2001) The Alzheimer amyloid precursor protein (APP) and FE65, an APP-binding protein, regulate cell movement. *J. Cell Biol.* **153,** 1403–1414
16. Cao, X., and Sudhof, T. C. (2001) A transcriptionally [correction of transcriptively] active complex of APP with Fe65 and histone acetyltransferase Tip60. *Science* **293,** 115–120
17. Perkinton, M. S., Standen, C. L., Lau, K. F., Kesavapany, S., Byers, H. L., Ward, M., McLoughlin, D. M., and Miller, C. C. (2004) The c-Abl tyrosine kinase phosphorylates the Fe65 adaptor protein to stimulate Fe65/amyloid precursor protein nuclear signaling. *J. Biol. Chem.* **279,** 22084–22091
18. Okamoto, M., and Sudhof, T. C. (1997) Mint, Munc 18-interacting proteins in synaptic vesicle exocytosis. *J. Biol. Chem.* **272,** 31459–31464
19. Borg, J. P., Straight, S. W., Kaech, S. M., de Taddeo-Borg, M., Kroon, D. E., Karnak, D., Turner, R. S., Kim, S. K., and Margolis, B. (1998) Identification of an evolutionarily conserved heterotrimeric protein complex involved in protein targeting. *J. Biol. Chem.* **273,** 31633–31636
20. Sastre, M., Turner, R. S., and Levy, E. (1998) X11 interaction with beta-amyloid precursor protein modulates its cellular stabilization and reduces amyloid beta-protein secretion. *J. Biol. Chem.* **273,** 22351–22357
21. Tomita, S., Ozaki, T., Taru, H., Oguchi, S., Takeda, S., Yagi, Y., Sakiyama, S., Kirino, Y., and Suzuki, T. (1999) Interaction of a neuron-specific protein containing PDZ domains with Alzheimer's amyloid precursor protein. *J. Biol. Chem.* **274,** 2243–2254
22. He, X., Cooley, K., Chung, C. H., Dashti, N., and Tang, J. (2007) Apolipoprotein receptor 2 and X11 α/β mediate apolipoprotein E-induced endocytosis of amyloid-β precursor protein and beta-secretase, leading to amyloid-beta production. *J. Neurosci.* **27,** 4052–4060
23. Hoe, H. S., and Rebeck, G. W. (2005) Regulation of ApoE receptor proteolysis by ligand binding. *Brain Res. Mol. Brain Res.* **137,** 31–39
24. Soule, H. D., Maloney, T. M., Wolman, S. R., Peterson, W. D., Jr., Brenz, R., McGrath, C. M., Russo, J., Pauley, R. J., Jones, R. F., and Brooks, S. C. (1990) Isolation and characterization of a spontaneously immortalized human breast epithelial cell line, MCF-10. *Cancer Res.* **50,** 6075–6086
25. Pak, D. T., Yang, S., Rudolph-Correia, S., Kim, E., and Sheng, M. (2001) Regulation of dendritic spine morphology by SPAR, a PSD-95-associated RapGAP. *Neuron* **31,** 289–303
26. Borg, J. P., Ooi, J., Levy, E., and Margolis, B. (1996) The phosphotyrosine interaction domains of X11 and FE65 bind to distinct sites on the YENPTY motif of amyloid precursor protein. *Mol. Cell. Biol.* **16,** 6229–6241
27. Hoe, H. S., Minami, S. S., Makarova, A., Lee, J., Hyman, B. T., Matsuoka, Y., and Rebeck, G. W. (2008) Fyn modulation of Dab1 effects on amyloid precursor protein and ApoE receptor 2 processing. *J. Biol. Chem.* **283,** 6288–6299
28. Herz, J. (2009) Apolipoprotein E receptors in the nervous system. *Curr. Opin. Lipidol.* **20,** 190–196
29. Trommsdorff, M., Gotthardt, M., Hiesberger, T., Shelton, J., Stockinger, W., Nimpf, J., Hammer, R. E., Richardson, J. A., and Herz, J. (1999) Reeler/Disabled-like disruption of neuronal migration in knockout mice lacking the VLDL receptor and ApoE receptor 2. *Cell* **97,** 689–701
30. Mayer, H., Duit, S., Hauser, C., Schneider, W. J., and Nimpf, J. (2006) Reconstitution of the Reelin signaling pathway in fibroblasts demonstrates that Dab1 phosphorylation is independent of receptor localization in lipid rafts. *Mol. Cell. Biol.* **26,** 19–27
31. Lau, K. F., McLoughlin, D. M., Standen, C. L., Irving, N. G., and Miller, C. C. (2000) Fe65 and X11beta co-localize with and compete for binding to the amyloid precursor protein. *Neuroreport* **11,** 3607–3610
32. Parisiadou, L., and Efthimiopoulos, S. (2007) Expression of mDab1 promotes the stability and processing of amyloid precursor protein and this effect is counteracted by X11alpha. *Neurobiol. Aging* **28,** 377–388
33. Lee, J. H., Lau, K. F., Perkinton, M. S., Standen, C. L., Shemilt, S. J., Mercken, L., Cooper, J. D., McLoughlin, D. M., and Miller, C. C. (2003) The neuronal adaptor protein X11alpha reduces Abeta levels in the brains of Alzheimer's APPswe Tg2576 transgenic mice. *J. Biol. Chem.* **278,** 47025–47029
34. Lee, J. H., Lau, K. F., Perkinton, M. S., Standen, C. L., Rogelj, B., Falinska, A., McLoughlin, D. M., and Miller, C. C. (2004) The neuronal adaptor protein X11beta reduces amyloid beta-protein levels and amyloid plaque formation in the brains of transgenic mice. *J. Biol. Chem.* **279,** 49099–49104
35. Mueller, H. T., Borg, J. P., Margolis, B., and Turner, R. S. (2000) Modulation of amyloid precursor protein metabolism by X11alpha/Mint-1. A deletion analysis of protein-protein interaction domains. *J. Biol. Chem.* **275,** 39302–39306
36. Chen, W. J., Goldstein, J. L., and Brown, M. S. (1990) NPXY, a sequence often found in cytoplasmic tails, is required for coated pit-mediated internalization of the low density lipoprotein receptor. *J. Biol. Chem.* **265,** 3116–3123
37. Vishnu, S., Hertenstein, A., Betschinger, J., Knoblich, J. A., Gert de Couet, H., and Fischbach, K. F. (2006) The adaptor protein X11Lα/Dmint1 interacts with the PDZ-binding domain of the cell recognition protein Rst in *Drosophila*. *Dev. Biol.* **289,** 296–307
38. Penzes, P., Johnson, R. C., Sattler, R., Zhang, X., Huganir, R. L., Kambampati, V., Mains, R. E., and Eipper, B. A. (2001) The neuronal Rho-GEF Kalirin-7 interacts with PDZ domain-containing proteins and regulates dendritic morphogenesis. *Neuron* **29,** 229–242
39. Hack, I., Hellwig, S., Junghans, D., Brunne, B., Bock, H. H., Zhao, S., and Frotscher, M. (2007) Divergent roles of ApoER2 and Vldlr in the migration of cortical neurons. *Development* **134,** 3883–3891

Received for publication May 28, 2009.
Accepted for publication August 6, 2009.